Cancer Management and Research

Elevate Series

Open Access Full Text Article

ORIGINAL RESEARCH

CircCDK6 Regulates Stemness Maintenance and Cisplatin Resistance in Lung Adenocarcinoma via the Wnt/β-Catenin Signaling Pathway

Dan Li[1], Yanwei Shen[2], Li Wang[1], Huan Sun[1], Yuan Wang[3]

[1]Department of Respiratory and Critical Care Medicine, The First Affiliated Hospital of Xi'an Jiaotong University, Xi'an, Shaanxi, 710061, People's Republic of China; [2]Department of Surgical Oncology, Shaanxi Provincial People's Hospital, Xi'an, Shaanxi, 710061, People's Republic of China; [3]Department of Medical Imaging, The First Affiliated Hospital of Xi'an Jiaotong University, Xi'an, Shaanxi, 710061, People's Republic of China

Correspondence: Yuan Wang, Department of Medical Imaging, The First Affiliated Hospital of Xi'an Jiaotong University, No. 277, Yanta West Road, Yanta District, Xi'an, Shaanxi, 710061, People's Republic of China, Email wangyuan8003@eyou.com

Objective: This study investigates the role of circCDK6 in maintaining cancer stem cell (CSC) properties and mediating cisplatin resistance in lung adenocarcinoma (LUAD), with a focus on the involvement of the Wnt/β-catenin signaling pathway.

Methods: The expression levels of circCDK6 in various LUAD cell lines were measured using quantitative real-time PCR. Gain- and loss-of-function experiments were conducted by plasmid-mediated overexpression and siRNA-mediated knockdown of circCDK6. Cisplatin sensitivity was assessed using the Cell Counting Kit-8 assay and colony formation assay. The involvement of the Wnt/β-catenin pathway was examined by inhibiting the pathway with IWR-1. A subcutaneous xenograft model in BALB/c nude mice was used to evaluate the in vivo effects of circCDK6 knockdown on cisplatin responsiveness, and tumor tissues were analyzed through hematoxylin and eosin staining and immunohistochemistry for Ki-67 expression.

Results: CircCDK6 expression was significantly elevated in H1299 and H1975 cells compared to A549 and PC-9 cells. Overexpression of circCDK6 increased stemness markers, such as CD133, Oct4, and Sox2, and enhanced cisplatin resistance, as demonstrated by higher IC_{50} values and increased colony formation. In contrast, circCDK6 silencing significantly reduced cisplatin resistance. Western blot analysis revealed that circCDK6 activated the Wnt/β-catenin pathway by upregulating Axin2, β-catenin, and c-Myc. In vivo, circCDK6 knockdown reduced tumor volume, improved the anti-tumor effect of cisplatin, and decreased Ki-67 expression.

Conclusion: CircCDK6 may promote CSC properties and contribute to cisplatin resistance in LUAD, potentially through activation of the Wnt/β-catenin pathway. These findings suggest that circCDK6 may represent a potential therapeutic target for overcoming chemoresistance in LUAD, although further studies are needed to validate its role and clinical relevance.

Keywords: cancer stem cell-like properties, chemoresistance mechanisms, noncoding RNA, lung cancer progression, β-catenin signaling

Introduction

Lung adenocarcinoma (LUAD) is the most common subtype of non-small cell lung cancer (NSCLC), accounting for more than 40% of all lung cancer cases.[1] With changes in global smoking patterns and increasing environmental pollution, the incidence of LUAD has risen significantly over the past decades, particularly among women and non-smokers.[2] The etiology of LUAD is multifactorial, involving genetic predisposition, environmental influences, and individual characteristics.[3,4] Prolonged exposure to secondhand smoke and air pollution has been identified as major environmental risk factors for LUAD development.[5,6] LUAD is often asymptomatic in its early stages, making early diagnosis particularly challenging. As a result, many patients are diagnosed at advanced stages of the disease.[7] Although recent advances in imaging technologies and molecular biomarkers have improved early detection, substantial challenges remain in the implementation and accessibility of effective screening strategies, especially among high-risk populations.[8] Currently, cisplatin remains one of the standard chemotherapeutic agents for LUAD. However, as treatment progresses, a growing number of patients develop resistance to cisplatin, significantly compromising therapeutic outcomes.[9] This

https://doi.org/10.2147/CMAR.S588277
Received: 11 December 2025
Accepted: 29 April 2026
Published: 15 May 2026

resistance is not only associated with genetic mutations within tumor cells but is also closely linked to the presence of cancer stem cells (CSCs), which play crucial roles in tumor initiation, progression, and chemoresistance.[10] Therefore, elucidating the molecular mechanisms underlying CSC-associated stemness in LUAD may offer novel insights into overcoming chemotherapy resistance.

Circular RNAs (circRNAs) are a class of non-coding RNAs characterized by a covalently closed loop structure. Emerging evidence indicates that circRNAs participate in tumorigenesis, cancer progression, and chemoresistance.[11] Numerous studies have demonstrated that circRNAs play essential roles in regulating tumor cell proliferation, migration, invasion, and the maintenance of stemness across various cancer types.[12] Recent studies have reported that circCDK6 is dysregulated in human cancers. For example, in cervical cancer, circCDK6 suppresses tumor proliferation and metastasis by acting as a sponge for miR-449a.[13] However, the role and mechanism of circCDK6 in LUAD remain unexplored. Notably, the Wnt/β-catenin signaling pathway is a well-established regulator of cellular processes such as proliferation, differentiation, and migration, and it is implicated in the pathogenesis of multiple cancers.[14,15] Importantly, in the context of cisplatin resistance, Wnt/β-catenin signaling has been identified as a critical modulator that may influence chemotherapy outcomes by altering CSC characteristics and drug resistance mechanisms.[15,16]

This study aims to clarify whether circCDK6 contributes to cisplatin resistance in LUAD through the Wnt/β-catenin signaling pathway. By exploring the interaction between circCDK6 and the Wnt/β-catenin signaling pathway, this study seeks to elucidate how circCDK6 contributes to chemoresistance and to identify potential therapeutic targets for overcoming treatment failure in LUAD.

Materials and Methods

Cell and Culture Conditions

Human LUAD cell lines A549 (Pricella, CL-0016), H1299 (Pricella, CL-0165), H1975 (Pricella, CL-0298), and PC-9 (Pricella, CL-0668) were used in this study. All cell lines were authenticated by short tandem repeat (STR) profiling (Wuhan Pricella Biotechnology Co., Ltd.) and confirmed to match the reference profiles for each line. All cells were cultured in RPMI-1640 medium (Gibco, 31870082) supplemented with 10% fetal bovine serum (FBS; Gibco, 30067–334) and 1% penicillin-streptomycin solution (Gibco, 15140122) in a humidified incubator at 37°C with 5% CO_2. Cells were subcultured when they reached 80% confluency.

Cell Transfection and Treatment

circCDK6 overexpression plasmids were transfected into A549 cells, while siRNAs targeting circCDK6 were transfected into H1299 cells for functional assays. Cells were transfected using Lipofectamine 2000 reagent (Invitrogen, 11668019) according to the manufacturer's instructions. For each well, 2 μg of circCDK6 overexpression plasmid (Origene) or small interfering RNA (siRNA) oligonucleotides (Guangzhou Anernor Biotechnology Co., Ltd.) were used. The siRNAs were designed to specifically target the back-splice junction of human circCDK6 (hsa_circ_0001724) according to the annotation provided by circBase (https://www.circbase.org/cgibin/singlerecord.cgi?id=hsa_circ_0001724). The specificity of the siRNAs was confirmed using NCBI BLAST to avoid off-target binding to the linear CDK6 transcript (RefSeq: NM_001259.8). The sequences were as follows: si-circCDK6 #1: AAGUUUUAGCAGAAAACCUCUTT; si-circCDK6 #2: CCAAGUUUUAGCAGAAAACCUTT; negative control siRNA (si-NC): AUGUUUAAAUUGUUGUGAAATT. The mixtures were incubated for 4 h, after which the medium was replaced with fresh culture medium and incubated for an additional 48 h prior to subsequent experiments.

For Wnt/β-catenin pathway inhibition, after 48 h of transfection with circCDK6 overexpression plasmids, cells were treated with 10 μM IWR-1 (Selleck, S7086) for 24 h,[17] followed by cisplatin treatment for the CCK-8 assay. Cisplatin (Sigma-Aldrich, P4394) was applied at concentrations of 0, 2, and 4 μM for 48 h prior to colony formation assays of A549 and H1299 cells. For RNase R validation of circCDK6, total RNA from A549 cells was treated with 3 U/μg RNase R (Epicenter Technologies) at 37°C for 30 min, followed by analysis of the expression levels of circular and linear transcripts.

Quantitative Real-Time PCR (qRT-PCR)

When cells reached approximately 70% confluence, total RNA was extracted using TRIzol reagent (Invitrogen, 15596026), and reverse transcription was performed using a reverse transcription kit (Thermo Fisher, K1622). qPCR was carried out using SYBR Green PCR Master Mix (Takara, RR820A) under the following thermal cycling conditions: initial denaturation at 95°C for 5 min, followed by 40 cycles of 95°C for 15s, 60°C for 30s, and 72°C for 30s. GAPDH was used as the internal control, and relative expression levels were calculated using the $2^{-\Delta\Delta Ct}$ method. The primer sequences were as follows: circCDK6 forward: 5′-CCAAGTTTTAGCAGAAAACCTCTCC-3′; circCDK6 reverse: 5′-CTCCTCGAAGCGAAGTCCTC-3′; linear CDK6 forward: 5′-CAGTGACTTTCCTCTGACATGC-3′; linear CDK6 reverse: 5′-GGCTCTGCATAAAACGGCAC-3′; GAPDH forward: 5′-CCAGGTGGTCTCCTCTGA-3′; GAPDH reverse: 5′-GCTGTAGCCAAATTCGTTG-3′.

Western Blot

Cells were lysed in RIPA buffer (Beyotime, P0013B), and protein concentration was determined using the BCA Protein Assay Kit (Thermo Fisher, 23227). Equal amounts of protein (30 μg per sample) were separated by 12% SDS-PAGE and transferred to PVDF membranes (Millipore, IPVH00010). After blocking, membranes were incubated overnight at 4°C with the following primary antibodies: CD133 (Abcam, ab222782, 1:2000), Oct4 (Abcam, ab137427, 1:1000), Sox2 (Abcam, ab171380, 1:1000), p-β-catenin (Abcam, ab314450, 1:1000), β-catenin (Abcam, ab68183, 1:1000), c-Myc (Abcam, ab19312, 1:1000), Axin2 (Abcam, ab109307, 1:1000), p-GSK3β (Abcam, ab68476, 1:1000), and GSK3β (Abcam, ab93926, 1:1000). GAPDH (Abcam, ab8245, 1:1000) was used as the loading control. HRP-conjugated secondary antibodies (Abcam, ab6721, 1:2000) were applied, and immunoreactive bands were visualized using an enhanced chemiluminescence detection kit (Thermo Fisher, 34577). Densitometric analysis was performed using ImageJ software (National Institutes of Health).

CCK-8 Assay for Cell Viability

Cell viability was assessed using the Cell Counting Kit-8 (CCK-8; Dojindo, CK04). Cells were seeded in 96-well plates at a density of 4×10^3 cells/well. After 24 h of adherence, the medium was replaced with fresh medium containing varying concentrations of cisplatin (0, 1, 2, 4, 8, 16, and 32 μM). After 48 h of incubation, 10 μL of CCK-8 reagent was added to each well and incubated at 37°C for 1.5 h. Absorbance was measured at 450 nm using a microplate reader (BioTek, ELx800). Each group included three replicate wells, and blank wells were used for background correction. Dose-response curves and IC_{50} values were generated using GraphPad Prism 9.0.

Colony Formation Assay

The colony formation assay was used to evaluate the proliferative capacity of LUAD cells following cisplatin treatment. A549 and H1299 cells were treated with 0, 2, or 4 μM cisplatin and cultured for 10–14 days, with medium refreshed every 3 days. Colonies were fixed with 4% paraformaldehyde (Solarbio, P1110) for 15 min and stained with 0.1% crystal violet (Beyotime, C0121) for 20 min. After thorough rinsing and air drying, colonies were imaged and quantified using ImageJ.

Animal Housing

Eighteen 4–5-week-old male BALB/c nude mice (SM-014), weighing 20–25 g, were obtained from Shanghai Model Organisms Center, Inc. All animals were housed under standard conditions at 22 ± 2°C with 60% humidity and a 12 h light/dark cycle, with ad libitum access to food and water. All animal procedures were conducted in compliance with the Regulations on the Administration of Laboratory Animals, performed in accordance with the Guide for the Care and Use of Laboratory Animals (NIH). The animal study protocol was approved by the Animal Ethics Committee of the Health Science Center of Xi'an Jiaotong University (Approval No. XJTUAE2023-1998, 19 June 2023). This study is reported in accordance with the ARRIVE guidelines.

Animal Model

To establish subcutaneous tumor xenografts, 1×10^6 H1299 cells in 0.1 mL PBS were injected into the right axilla of BALB/c nude mice. Tumor length and width were measured weekly using calipers, and tumor volume was calculated as (length × width^2)/2. Once tumors reached approximately 100 mm^3 in volume, mice were randomly divided into three groups (n = 6 per group): (1) si-NC, (2) si-NC + cisplatin (DDP), and (3) si-circCDK6 #1 + DDP. Mice in the si-NC + DDP group were intraperitoneally injected with 5 mg/kg cisplatin (Sigma-Aldrich, P4394) twice weekly.[18] Additionally, based on superior knockdown efficiency and functional validation in vitro, si-circCDK6 #1 was selected for in vivo xenograft experiments. Mice in the si-circCDK6 #1 + DDP group received 5 mg/kg cisplatin together with si-circCDK6 #1 lentivirus (1×10^8 TU in 100 μL PBS) via tail vein injection once per week starting on the first day of treatment. Lentiviral injection was initiated on the first day of cisplatin treatment and repeated weekly to ensure sustained gene silencing throughout the treatment period. The si-NC group received si-NC lentivirus (1×10^8 TU in 100 μL PBS) via tail vein injection once per week and served as the negative control. Mice in the si-NC + DDP group received si-NC lentivirus together with intraperitoneal cisplatin treatment.

Tumor growth inhibition (TGI) was calculated based on the change in tumor volume from baseline (week 1) to endpoint (week 4), as previously described.[19] TGI (%) was calculated as $[1 - (Tt - T0)/(Ct - C0)] \times 100$, where Tt and T0 represent the mean tumor volumes of the treatment group at the study endpoint and baseline, respectively, and Ct and C0 represent the mean tumor volumes of the reference control group at the study endpoint and baseline, respectively. In this study, TGI was calculated for both the si-NC + DDP group relative to the si-NC group and the si-circCDK6 #1 + DDP group relative to the si-NC + DDP group to quantify the antitumor effect of cisplatin and the additional sensitizing effect of circCDK6 knockdown. After 4 weeks of treatment, all mice were euthanized by intraperitoneal injection of sodium pentobarbital (100 mg/kg; Sigma-Aldrich, P3761), and tumors were harvested, photographed, and weighed.

Hematoxylin and Eosin (HE) Staining

Tumor tissues were fixed in 4% paraformaldehyde (Servicebio, G1101) for 24 h, dehydrated with graded ethanol, cleared in xylene (Sinopharm, 10023418), and embedded in paraffin. Sections of 4 μm thickness were cut (Leica RM2235), deparaffinized, rehydrated, and stained with hematoxylin (Servicebio, G1004) for 5 min, differentiated in 1% acid alcohol, blued in 0.2% ammonia water, counterstained with eosin (Servicebio, G1001) for 2 min, dehydrated, cleared, and mounted. Images were acquired using a bright-field microscope (Olympus BX53).

Immunohistochemistry (IHC) Staining

Paraffin-embedded tumor sections (4 μm) were deparaffinized, rehydrated, and subjected to antigen retrieval in sodium citrate buffer (pH 6.0; Servicebio, G1202). Endogenous peroxidase activity was blocked with 3% hydrogen peroxide (Servicebio, G0115), followed by blocking with 5% BSA (Sigma-Aldrich, A7906). Sections were incubated overnight at 4°C with rabbit monoclonal anti-Ki-67 antibody (1:200; Abcam, ab16667), then with HRP-conjugated secondary antibody (1:500; Servicebio, G1213) for 30 min. Staining was developed with DAB (Servicebio, G1212) and counterstained with hematoxylin (Servicebio, G1004), dehydrated, cleared, and mounted. Representative images were obtained under a bright-field microscope (Olympus BX53). For semi-quantitative analysis of Ki-67 staining, digital images were analyzed using ImageJ software (National Institutes of Health). Ki-67-positive cells were quantified as the percentage of Ki-67-positive tumor cells among total tumor cells in randomly selected high-power fields.

Bioinformatic Prediction of circCDK6-Associated miRNAs and Wnt Targets

To explore potential upstream mechanisms by which circCDK6 may regulate Wnt/β-catenin signaling, an in silico bioinformatic analysis was performed. The circRNA annotation of circCDK6 was obtained from circBase (https://www.circbase.org/) using hsa_circ_0001724 as the reference entry. Candidate miRNAs potentially binding to circCDK6 and their putative binding sites were predicted using CircInteractome (https://circinteractome.nia.nih.gov/). Wnt pathway-related genes were collected from the KEGG Wnt signaling pathway dataset (hsa04310). Putative target genes of the candidate miRNAs were then screened using TargetScanHuman 8.0 (https://www.targetscan.org/vert_80/), and the

intersection between predicted miRNA targets and Wnt pathway components was identified to construct a circCDK6–miRNA–Wnt regulatory network.

To provide external support for the potential association between circCDK6 and Wnt/β-catenin signaling in LUAD, publicly available TCGA-LUAD transcriptomic data were additionally analyzed. Because circRNA expression data were unavailable in the TCGA dataset, CDK6 was used as a proxy for circCDK6. CDK6 expression was compared between paired tumor and adjacent normal tissues. In addition, Pearson correlation analysis was performed between CDK6 and representative Wnt/β-catenin pathway-related genes, including CTNNB1, MYC, LEF1, TCF7, TCF7L2, GSK3B, and APC. The correlation coefficients were visualized as a heatmap.

Statistical Analysis

All data were expressed as mean ± standard deviation (SD). Statistical analyses were performed using GraphPad Prism 9.0 (GraphPad Software, San Diego, CA, USA). Comparisons between two groups were made using two-tailed Student's t-tests. For multiple group comparisons, one-way or two-way analysis of variance (ANOVA) followed by Tukey's post hoc test was used. IC_{50} values were calculated by nonlinear regression based on dose-response curves. $p < 0.05$ was considered statistically significant.

Results

CircCDK6 Is Associated with Maintaining Stemness Properties of LUAD Cells by Regulating the Expression of Stemness Markers

In A549 cells, circCDK6 remained stable after RNase R treatment, whereas linear mRNA was significantly degraded, confirming the circular structure and resistance to exonuclease degradation of circCDK6 (Figure 1A). qRT-PCR analysis revealed that circCDK6 expression was higher in H1299 and H1975 cells than in A549 and PC-9 cells (Figure 1B). Transfection of H1299 cells with circCDK6-specific siRNAs significantly reduced circCDK6 expression, validating the knockdown efficiency (Figure 1C). Concurrently, silencing circCDK6 resulted in marked downregulation of stemness-related proteins including CD133, Oct4, and Sox2 (Figure 1D), suggesting that circCDK6 may promote the expression of stemness markers. In contrast, circCDK6 overexpression in A549 cells significantly increased circCDK6 levels (Figure 1E) and led to upregulation of CD133, Oct4, and Sox2 (Figure 1F), further supporting its positive regulatory role in stemness maintenance.

CircCDK6 Expression is Associated with Altered Cisplatin Sensitivity in LUAD Cells

CCK-8 assay demonstrated that A549 cells overexpressing circCDK6 exhibited enhanced resistance to cisplatin, with the IC_{50} value increasing from 4.263 μM in the control group to 10.18 μM. Conversely, in H1299 cells, transfection with si-circCDK6 #1 and si-circCDK6 #2 significantly increased cisplatin sensitivity, with IC_{50} values decreasing from 10.59 μM in the control group to 2.594 μM and 1.622 μM, respectively (Figure 2A, B and Table 1). Colony formation assays showed that, under different concentrations of cisplatin, the number of colonies formed by OE-circCDK6 cells was higher than that of the control group, indicating enhanced cell survival (Figure 2C). In contrast, colony numbers in si-circCDK6 #1 and si-circCDK6 #2 groups were significantly reduced in H1299 cells, and the reduction was more pronounced with increasing cisplatin concentrations (Figure 2D). These results indicate that circCDK6 upregulation decreases cisplatin sensitivity, whereas its silencing enhances drug responsiveness.

CircCDK6 Expression Correlates with Wnt/β-Catenin Signaling Activity and Cisplatin Response

Western blot analysis showed that overexpression of circCDK6 significantly increased the protein levels of Axin2, β-catenin, and c-Myc, while the levels of p-β-catenin and p-GSK3β were markedly decreased. Total GSK3β expression remained unchanged (Figure 3A). In CCK-8 assays, the IC_{50} value in the OE-circCDK6 + DMSO group was 13.36 μM, significantly higher than that of the NC group (3.351 μM). Notably, treatment with the Wnt pathway inhibitor IWR-1

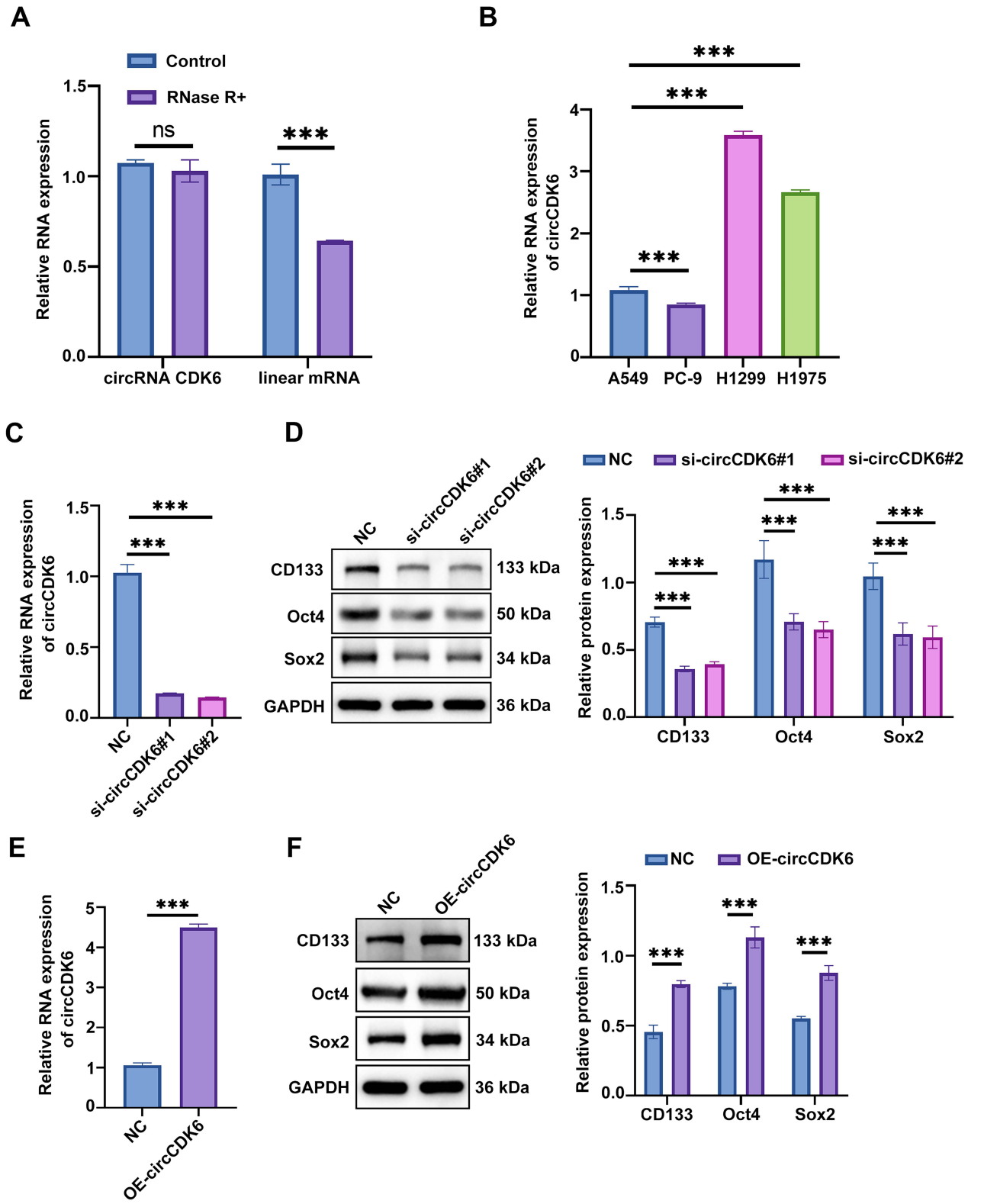

Figure 1 CircCDK6 is associated with maintaining stemness properties of LUAD cells by regulating the expression of stemness markers. (**A**) qRT-PCR analysis of circCDK6 and linear CDK6 mRNA stability following RNase R treatment. (**B**) Relative expression levels of circCDK6 in various LUAD cell lines measured by qRT-PCR. (**C**) Knockdown efficiency of circCDK6 in H1299 cells after siRNA transfection assessed by qRT-PCR. (**D**) Western blot analysis of stemness markers (CD133, Oct4, Sox2) after circCDK6 knockdown in H1299 cells. (**E**) Validation of circCDK6 overexpression in A549 cells using qRT-PCR. (**F**) Western blot analysis of CD133, Oct4, and Sox2 following circCDK6 overexpression in A549 cells.
Note: Data are presented as mean ± SD (n = 3). Compared to the NC group, ***$p < 0.001$.
Abbreviations: qRT-PCR, quantitative reverse transcription PCR; siRNA, small interfering RNA; OE, overexpression; NC, negative control; circCDK6, circular RNA CDK6; ns, not significant.

https://doi.org/10.2147/CMAR.S588277

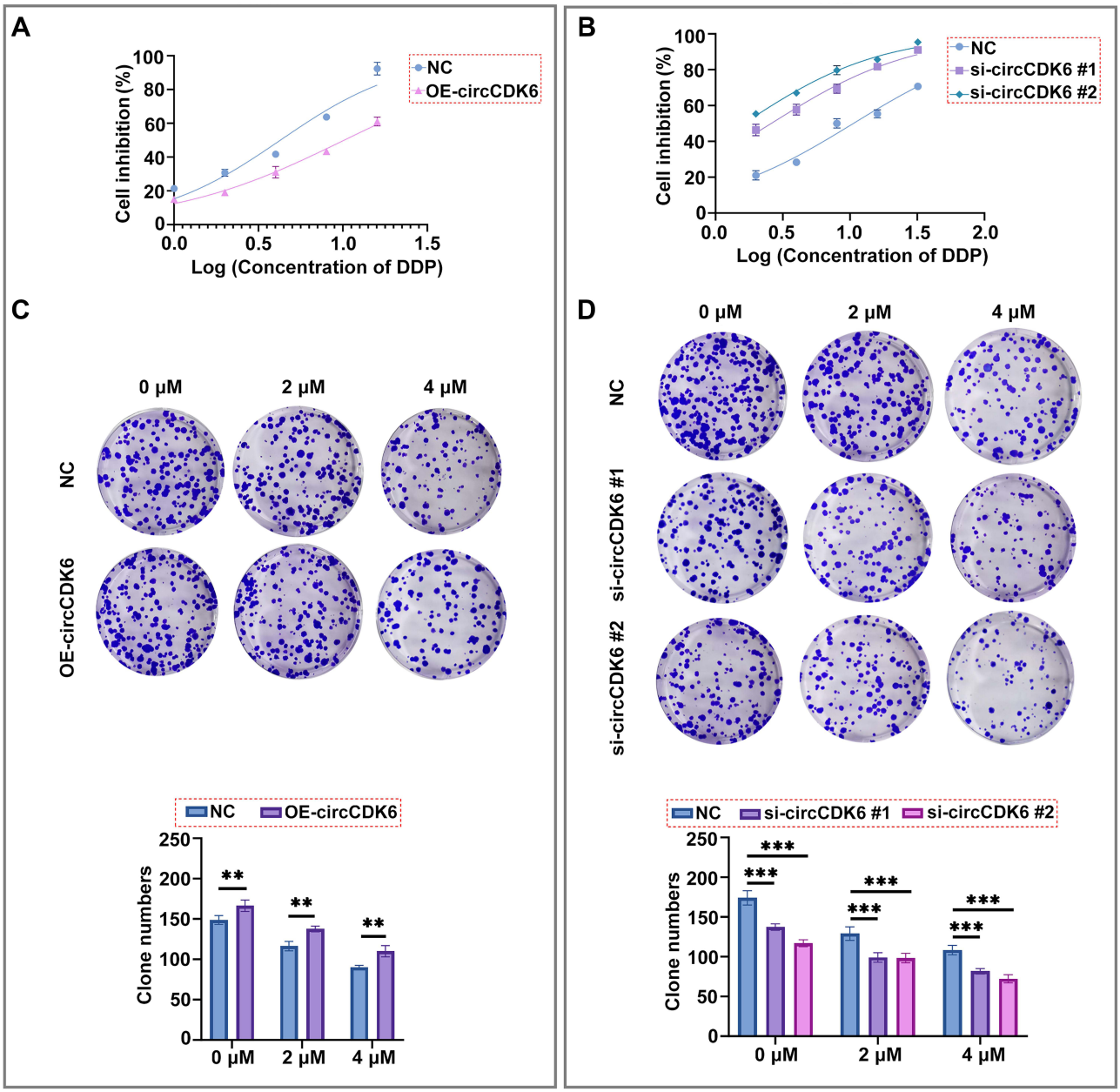

Figure 2 circCDK6 expression is associated with altered cisplatin sensitivity in LUAD cells. (**A**) Cell viability under different concentrations of DDP assessed in A549 cells using CCK-8 assay. Dose-response curves were plotted and IC_{50} values calculated. (**B**) Cell viability under different concentrations of DDP assessed in H1299 cells using CCK-8 assay. Dose-response curves were plotted and IC_{50} values calculated. (**C**) Colony formation assays under varying DDP concentrations in A549 cells, with representative staining images and quantification of colony numbers. (**D**) Colony formation assays under varying DDP concentrations in H1299 cells, with representative staining images and quantification of colony numbers. Data are shown as mean ± SD (n = 3). Compared to the NC group, $^{**}p < 0.01$, $^{***}p < 0.001$.
Abbreviations: CCK-8, Cell Counting Kit-8; DDP, cisplatin; NC, negative control; OE, overexpression; siRNA, small interfering RNA; IC_{50}, half maximal inhibitory concentration.

reduced the IC_{50} value to 5.080 μM in the OE-circCDK6 + IWR-1 group, indicating that circCDK6-mediated cisplatin resistance could be partially reversed by inhibiting the Wnt/β-catenin pathway (Figure 3B and Table 2).

CircCDK6 Knockdown Is Associated with Improved in Vivo Efficacy of Cisplatin in LUAD

Tumor volume assessment showed that tumor volumes in mice treated with si-circCDK6 combined with cisplatin were markedly smaller than those in the si-NC and si-NC + DDP groups (Figure 4A). Excised tumor tissues also demonstrated significantly reduced size in the si-circCDK6 #1 + DDP group (Figure 4B). Tumor weight measurements confirmed that

https://doi.org/10.2147/CMAR.S588277

Table 1 Best-Fit Parameters of Cisplatin Dose–Response Curves in A549 and H1299 Cells

Parameter	A549 NC	A549 OE-circCDK6	H1299 NC	H1299 si-circCDK6 #1	H1299 si-circCDK6 #2
$LogIC_{50}$	0.6297	1.008	1.025	0.4139	0.2100
HillSlope	1.179	0.8426	0.7957	0.8131	0.8462
IC_{50}	4.263	10.18	10.59	2.594	1.622

the average tumor mass in this group was significantly lower compared to controls (Figure 4C). Tumor volume monitoring over time revealed that the si-circCDK6 #1 + DDP group exhibited a pronounced reduction in growth rate from week 3, with the average volume at week 4 remaining below 300 mm^3, significantly smaller than in the other groups (Figure 4D). To further quantify the sensitizing effect of circCDK6 knockdown on cisplatin treatment in vivo, TGI was calculated based on changes in mean tumor volume from baseline (week 1) to endpoint (week 4). Compared with the si-NC group, the si-NC + DDP group showed a TGI of 55.57%. Importantly, when the si-NC + DDP group was used as the reference comparator, the si-circCDK6 #1 + DDP group showed a relative TGI of 81.98%, indicating that circCDK6 knockdown markedly enhanced the antitumor efficacy of cisplatin. In addition, the overall TGI of the si-circCDK6 #1 + DDP group relative to the si-NC group was 91.99% (Supplementary Table 1).

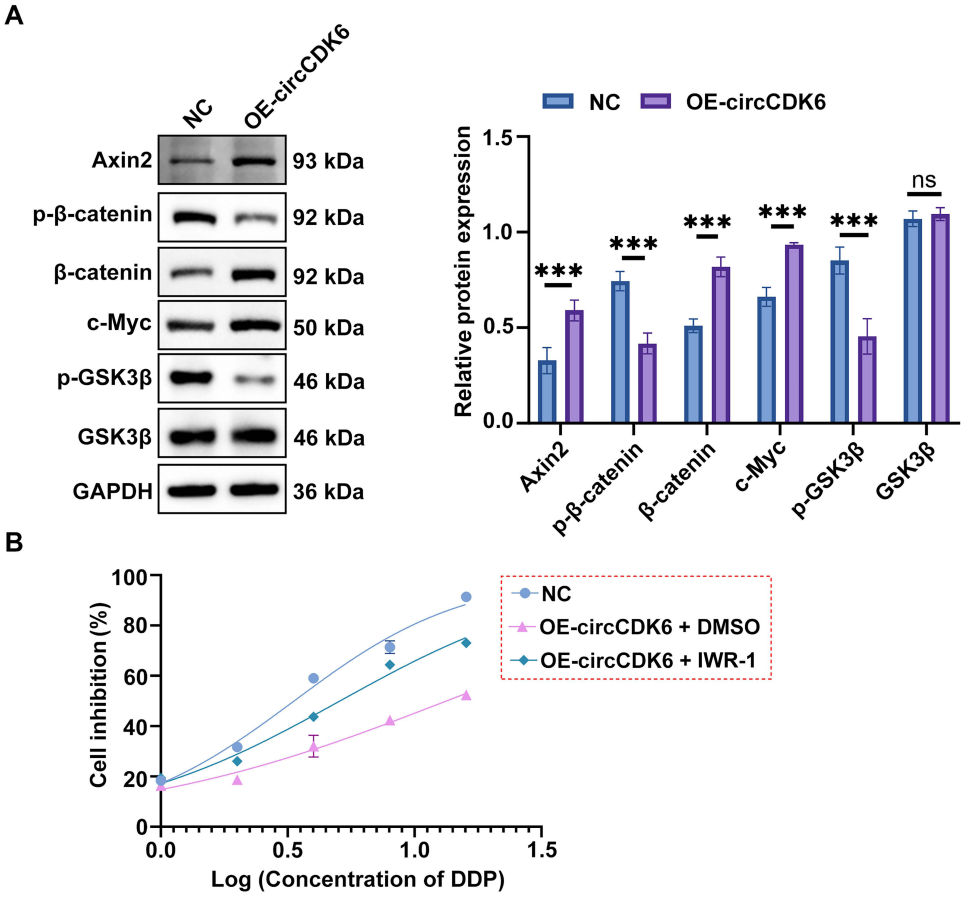

Figure 3 circCDK6 expression correlates with Wnt/β-catenin signaling activity and cisplatin response. (**A**) Western blot analysis of Axin2, total and phosphorylated β-catenin (p-β-catenin), c-Myc, total and phosphorylated GSK3β (p-GSK3β), with GAPDH as the loading control, in NC and OE-circCDK6 groups. (**B**) CCK-8 assay of cisplatin-induced growth inhibition in different treatment groups; dose-response curves and IC_{50} values are shown. Data are expressed as mean ± SD (n = 3). Compared to the NC group, ***$p < 0.001$; ns, not significant.

Abbreviations: NC, negative control; OE-circCDK6, circCDK6 overexpression; GSK3β, glycogen synthase kinase 3 beta; DDP, cisplatin; IWR-1, Wnt pathway inhibitor; CCK-8, Cell Counting Kit-8; GAPDH, glyceraldehyde-3-phosphate dehydrogenase.

https://doi.org/10.2147/CMAR.S588277

Table 2 Best-Fit Parameters of Cisplatin Dose–Response Curves in Cells with circCDK6 Overexpression and IWR-1 Treatment

Parameter	NC	OE-circCDK6 + DMSO	OE-circCDK6 + IWR-1
$LogIC_{50}$	0.5252	1.126	0.7059
HillSlope	1.298	0.6753	0.9671
IC_{50}	3.351	13.36	5.080

CircCDK6 Knockdown Combined with DDP Enhances Tumor Tissue Damage and Reduces Ki-67 Expression

HE staining showed that tumor tissues in the si-NC group exhibited densely arranged cells with deeply stained nuclei, whereas DDP treatment induced partial tissue destruction. Notably, tumors in the si-circCDK6 #1 + DDP group displayed marked disorganization of tissue architecture and reduced cell density (Figure 5A). Immunohistochemistry analysis of Ki-67 revealed high proliferative activity in the si-NC group, a moderate decrease upon DDP treatment, and a pronounced reduction in the si-circCDK6 combined with DDP group. Semi-quantitative analysis further confirmed that

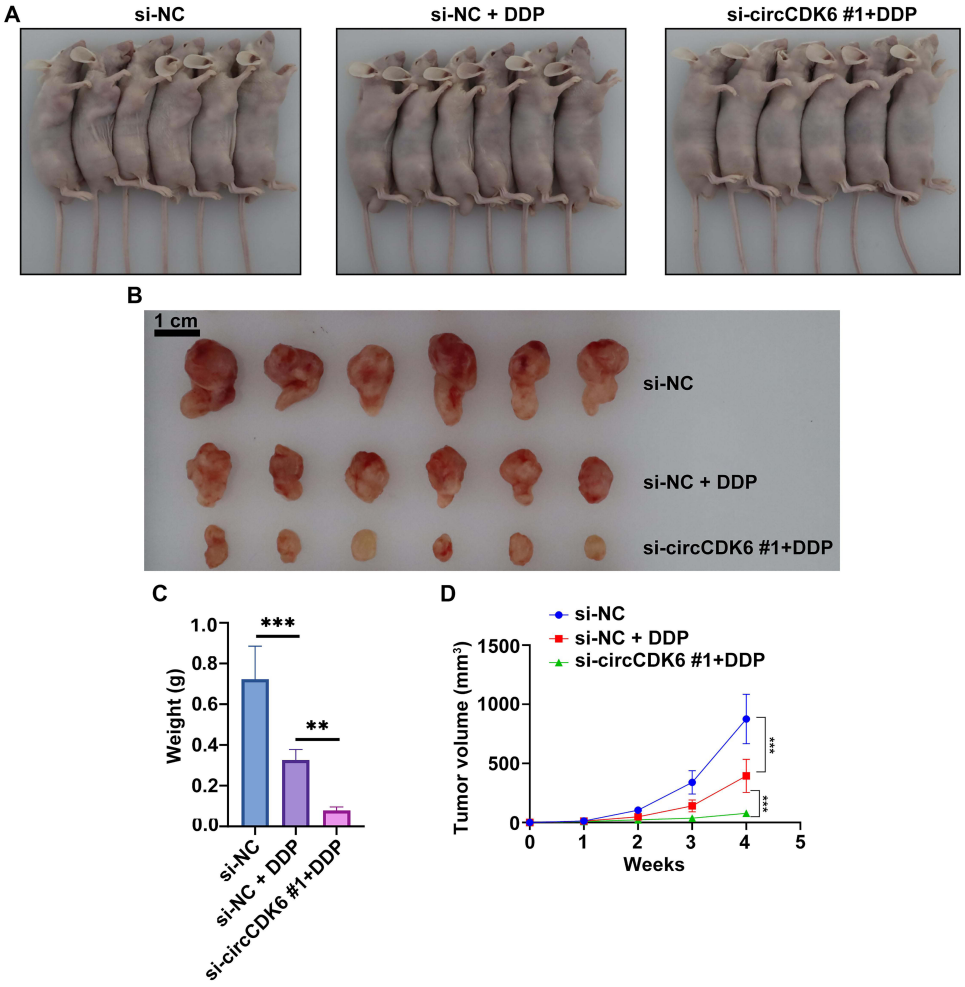

Figure 4 circCDK6 knockdown is associated with improved in vivo efficacy of cisplatin in LUAD. (**A**) Representative images of tumor-bearing mice in each treatment group. (**B**) Representative images of excised tumor tissues. (**C**) Tumor weight across groups. (**D**) Tumor growth curves measured weekly over the 4-week treatment period. Data are presented as mean ± SD (n = 6). Compared to the si-NC group, $^{**}p < 0.01$, $^{***}p < 0.001$.
Abbreviations: si-NC, negative control siRNA; si-circCDK6, circCDK6-targeting siRNA; DDP, cisplatin.

https://doi.org/10.2147/CMAR.S588277

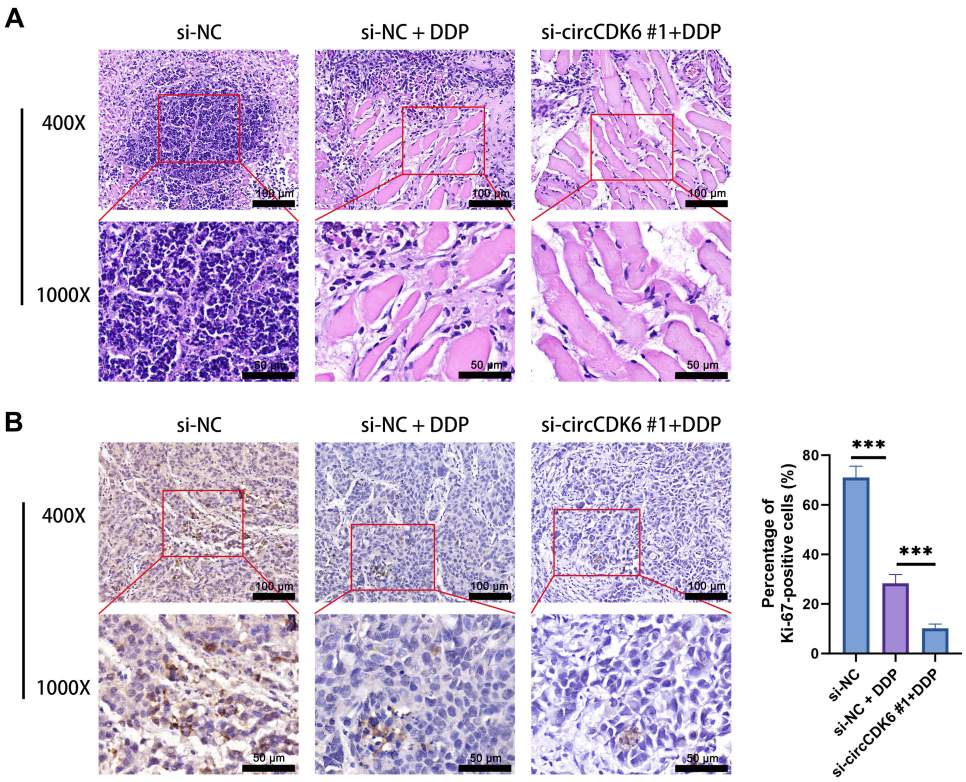

Figure 5 circCDK6 knockdown combined with DDP enhances tumor tissue damage and reduces Ki-67 expression. (**A**) Hematoxylin and eosin (HE) staining was performed to evaluate the morphological changes of tumor tissues under different treatments (scale bar = 100 μm, enlarge = 50 μm). (**B**) Immunohistochemistry (IHC) staining for Ki-67 was performed to assess proliferative activity in tumor tissues (scale bar = 100 μm, enlarge = 50 μm). Ki-67-positive cells were semi-quantitatively analyzed as the percentage of positively stained nuclei among total tumor cells. Data are presented as mean ± SD (n = 6). Compared to the si-NC group, ***$p < 0.001$.
Abbreviation: DDP, cisplatin.

the percentage of Ki-67-positive cells was markedly reduced in the si-circCDK6 #1 + DDP group compared with the si-NC and si-NC + DDP groups (Figure 5B).

Discussion

As the most prevalent subtype of NSCLC, LUAD is characterized by aggressive growth and high metastatic potential, with treatment resistance posing a major challenge to long-term chemotherapy efficacy. Accumulating evidence has demonstrated that CSCs play critical roles in LUAD initiation, progression, and resistance to chemotherapeutic agents such as cisplatin.[20–22] CSCs possess the capacity for self-renewal and multipotent differentiation, and are considered a key driver of tumor heterogeneity, recurrence, and therapy failure. For example, PHF5A has been shown to maintain CSC-like phenotypes in NSCLC by modulating HDAC8.[23] In line with this, our study revealed that circCDK6 was highly expressed in LUAD cell lines with pronounced stemness characteristics (H1299 and H1975). Moreover, knockdown of circCDK6 in H1299 cells significantly downregulated CD133, Oct4, and Sox2 expression, suggesting a potential role for circCDK6 in maintaining stemness in LUAD cells.

circRNAs, a class of non-coding RNAs with covalently closed-loop structures, are highly stable and have been implicated in cancer progression, stemness maintenance, metastasis, and drug resistance.[24,25] For instance, circ-EPB41 has been shown to sponge miR-486-3p, thereby increasing eIF5A expression and promoting the transcription of stemness-associated genes (SOX2, OCT4, NANOG, CD133) in lung CSCs.[26] Moreover, LUAD tissues frequently co-express core stemness genes such as OCT4, c-MYC, and SOX2, which may be regulated by the tumor microenvironment.[27] The regulation of CSC phenotypes and chemoresistance is tightly linked to several signaling pathways, particularly autophagy, Hedgehog, TGF-β, and Wnt/β-catenin.[28–30] In the present study, we demonstrated that circCDK6 promotes the expression of stemness markers in LUAD and activates the Wnt/β-catenin signaling

pathway, thereby enhancing cisplatin resistance. No previous studies have directly investigated the role of circCDK6 in lung cancer, particularly in relation to cisplatin resistance and its association with Wnt/β-catenin signaling. Previous studies have indicated that circRNAs can modulate CSC properties and participate in drug resistance, especially in the context of cisplatin. For example, circ-ZKSCAN1 promotes cisplatin resistance in NSCLC by targeting the miR-185-5p/TAGLN2 axis, and its knockdown restores cisplatin sensitivity and reduces proliferation, migration, and invasion.[31] Similarly, circ-PVT1 enhances cisplatin resistance in LUAD by regulating the miR-429/FOXK1 axis and inhibiting apoptosis.[32] These findings support the involvement of circRNAs in maintaining chemoresistant phenotypes, offering potential molecular targets for therapeutic intervention. Our data further confirmed that circCDK6 activates the Wnt/β-catenin pathway, as evidenced by increased expression of downstream effectors including β-catenin, Axin2, and c-Myc. In addition, analysis of the TCGA-LUAD dataset using CDK6 as a proxy for circCDK6 showed that CDK6 expression was not significantly different between paired tumor and normal tissues, but was positively correlated with several representative Wnt/β-catenin pathway-related genes, including CTNNB1, MYC, LEF1, TCF7, TCF7L2, GSK3B, and APC (Supplementary Figure 1). These findings provide external support for the proposed circCDK6-Wnt axis in LUAD. Notably, treatment with the Wnt pathway inhibitor IWR-1 partially reversed circCDK6-induced cisplatin resistance, supporting the mechanistic link between circCDK6 and this signaling axis.

Beyond drug resistance, the interaction between circRNAs and Wnt/β-catenin signaling has been widely implicated in cancer progression. For example, circZSWIM4 promotes LUAD progression by targeting miR-370-3p and miR-873-5p, which regulate FOXM1 and activate the Wnt/β-catenin pathway.[33] circCCND1 enhances NSCLC chemoresistance through miR-187-3p/FGF9 regulation and is linked to oxidative stress and Wnt pathway activation.[34] Additionally, hsa_circ_0018414 has been reported to inhibit LUAD progression by sponging miR-6807-3p and upregulating DKK1, thereby antagonizing Wnt/β-catenin signaling.[35]

Importantly, Wnt/β-catenin signaling has emerged as a key regulator of stemness maintenance and chemotherapy resistance across multiple cancers. In bladder cancer,[36] colorectal cancer,[37] and head and neck squamous cell carcinoma (HNSCC),[38] this pathway has been shown to mediate cisplatin resistance via CSC-related mechanisms. For example, LASS2 enhances cisplatin sensitivity by suppressing β-catenin dephosphorylation.[36] In colorectal cancer, miR-199a/b activates Wnt signaling by targeting GSK3β, thereby maintaining CSC-mediated cisplatin resistance.[37] In HNSCC, CD44 cooperates with β-catenin to drive cisplatin resistance.[38] In LUAD, Sox2 has been shown to sensitize cells to cisplatin by upregulating GSK3β and suppressing Wnt signaling activity. Together, these studies highlight Wnt/β-catenin signaling as a central axis linking CSC properties and chemoresistance.[39] This study is the first to report that circCDK6 can simultaneously modulate stemness and cisplatin resistance in LUAD through activation of the Wnt/β-catenin pathway. Compared with previously identified circRNAs such as circ-ZKSCAN1 and circ-PVT1 that modulate chemoresistance via miRNA axes,[31,32] our study suggests a potential mechanism of cisplatin resistance that may involve activation of the Wnt/β-catenin signaling pathway.

To further support this mechanistic hypothesis, we performed an additional bioinformatic analysis to predict miRNAs that may bind circCDK6 and regulate Wnt pathway-related genes (Supplementary File 1). CircInteractome-based analysis identified 11 candidate miRNAs potentially associated with circCDK6, and integration with KEGG Wnt signaling genes and TargetScanHuman 8.0 yielded 158 intersecting candidate target genes. As shown in Supplementary Figure 2A, the predicted targeting pattern was not uniformly distributed across all Wnt pathway genes. Instead, several candidate miRNAs, particularly miR-766, miR-1236, miR-1248, and miR-95, showed broader predicted connectivity with Wnt-related genes, and darker heatmap signals corresponded to more negative minimum cumulative weighted context++ scores, indicating stronger predicted targeting efficacy. Consistently, the integrated network in Supplementary Figure 2B highlighted recurrent downstream nodes including FZD3, APC2, WNT2B, MCC, WNT8B, GSK3B, PSEN1, and PRKCA. Together, these findings suggest that the potential ceRNA function of circCDK6 may involve multiple intermediate miRNAs converging on selected Wnt signaling components, rather than a single linear regulatory axis. Nevertheless, these results are based on in silico prediction and should be regarded as hypothesis-generating; direct experimental validation will be required in future studies.

Moreover, our in vivo data demonstrated that circCDK6 silencing significantly enhanced cisplatin-mediated tumor suppression in xenograft models, raising the possibility that circCDK6 could be explored as a translational target in future studies. In

addition to chemotherapy resistance, the tumor microenvironment (TME) is increasingly recognized as a critical determinant of therapeutic response, particularly in the setting of immunotherapy.[40] In LUAD and NSCLC, complex interactions among tumor cells, exhausted T cells, tumor-associated macrophages, dendritic cells, and stromal components shape immune surveillance and may influence sensitivity or resistance to immune checkpoint blockade.[41] Cytokine-mediated signaling is also an important component of this process, as inflammatory mediators such as IL-6 and related cytokine networks can promote an immunosuppressive microenvironment and contribute to reduced responsiveness to immunotherapy.[42] Moreover, tumor-associated macrophages and other suppressive immune populations may further impair antitumor immunity by interfering with T-cell function and supporting tumor progression in lung cancer.[43,44] Although the present study focused on cisplatin resistance rather than immunotherapy, these observations suggest that circCDK6-mediated stemness and Wnt/β-catenin activation may also have broader implications in shaping the TME and influencing future therapeutic responses, which warrants further investigation.

Despite these findings, some limitations remain. First, although bioinformatic analysis was performed to predict potential circCDK6-associated miRNAs and Wnt-related downstream targets, the interaction of circCDK6 with miRNAs or RNA-binding proteins was not experimentally validated. Second, the diagnostic or prognostic value of circCDK6 in LUAD was not assessed and warrants further investigation in clinical samples. Third, in vitro experiments lacked validation of linear CDK6 mRNA and protein expression to exclude off-target effects of siRNAs, and RNase R validation was only performed in A549 cells. Although the circular structure of circCDK6 was confirmed by RNase R treatment, we did not evaluate whether the siRNAs targeting the back-splice junction affected linear CDK6 mRNA or protein expression. Therefore, we could not fully exclude the possibility that part of the observed phenotype was influenced by alterations in the host gene CDK6. Fourth, the in vivo experiments did not include single-treatment arms, such as a si-circCDK6 monotherapy group, which limits the ability to distinguish the independent effect of circCDK6 knockdown on tumor growth from its potential chemosensitizing effect when combined with cisplatin. Moreover, molecular assessments such as immunohistochemistry for cleaved caspase-3 or β-catenin localization in xenograft tissues were not performed, limiting the mechanistic interpretation of in vivo findings. Lastly, the precise molecular mechanisms and the role of circCDK6 at different disease stages remain to be elucidated.

Conclusion

In summary, this work provides new insights into the molecular basis of LUAD recurrence and treatment failure and indicates that circCDK6 may represent a potential therapeutic target for overcoming chemoresistance in LUAD. This study suggests that circCDK6 may contribute to the maintenance of stemness and the promotion of cisplatin resistance through the Wnt/β-catenin pathway. Inhibition of this pathway can partially reverse these phenotypes, although further genetic and functional experiments are needed to confirm these findings.

Data Sharing Statement

The data that support the findings of this study are available from the corresponding author upon reasonable request.

Ethical Declarations

The animal study protocol was approved by the Animal Ethics Committee of the Health Science Center of Xi'an Jiaotong University (Approval No. XJTUAE2023-1998, 19 June 2023).

Author Contributions

All authors made a significant contribution to the work reported, whether that is in the conception, study design, execution, acquisition of data, analysis and interpretation, or in all these areas; took part in drafting, revising or critically reviewing the article; gave final approval of the version to be published; have agreed on the journal to which the article has been submitted; and agree to be accountable for all aspects of the work.

Funding

This study was supported by the Key Research and Development Program of Shaanxi (grant number 2025SF-YBXM-328 and 2024SF-YBXM-095), the Clinical Research Award of the First Affiliated Hospital of Xi'an Jiaotong University

(grant number XJTU1AF-CRF-2023-030 and XJTU1AF-CRF-2024-009), and Wu Jieping Medical Foundation Project (grant number 320.6750.2024-17-18).

Disclosure

The authors report no conflicts of interest in this work.

References

1. Hong JH, Park S, Kim H. et al. Volume and Mass Doubling Time of Lung Adenocarcinoma according to WHO Histologic Classification. *Korean J Radiol*. 2021;22(3):464–475. doi:10.3348/kjr.2020.0592
2. Forest F, Laville D, Da Cruz V, et al. WHO grading system for invasive pulmonary lung adenocarcinoma reveals distinct molecular signature: an analysis from the cancer genome atlas database. *Exp Mol Pathol*. 2022;125:104756. doi:10.1016/j.yexmp.2022.104756
3. Zhu Y, Wu Y, Zhu Z, et al. Residential greenness, air pollution, genetic predisposition and the risk of lung cancer. *Ecotoxicol Environ Saf*. 2025;294:118027. doi:10.1016/j.ecoenv.2025.118027
4. LoPiccolo J, Gusev A, Christiani DC, Jänne PA. Lung cancer in patients who have never smoked - an emerging disease. *Nat Rev Clin Oncol*. 2024;21(2):121–146. doi:10.1038/s41571-023-00844-0
5. Mochizuki A, Shiraishi K, Honda T, et al. Passive Smoking-Induced Mutagenesis as a Promoter of Lung Carcinogenesis. *J Thoracic Oncol*. 2024;19(7):984–994. doi:10.1016/j.jtho.2024.02.006
6. Jia Y, Ji Q, Zhang L, She Y, Su M, Shi Z. Prognosis of early-stage lung adenocarcinoma in young patients. *Clin Exp Pharmacol Physiol*. 2023;50 (10):826–832. doi:10.1111/1440-1681.13806
7. Fick CN, Dunne EG, Vanstraelen S, et al. High-risk features associated with recurrence in stage I lung adenocarcinoma. *J Thoracic Cardiovasc Surg*. 2025;169(2):436–444.e436. doi:10.1016/j.jtcvs.2024.05.009
8. Fick CN, Dunne EG, Toumbacaris N, et al. Late recurrence of completely resected stage I to IIIA lung adenocarcinoma. *J Thoracic Cardiovasc Surg*. 2025;169(2):445–453.e443. doi:10.1016/j.jtcvs.2024.06.026
9. Qu X, Ding T, Zhao H, Wang L. Epigenetic Regulation of RNF135 by LSD1 Promotes Stemness Maintenance and Brain Metastasis in Lung Adenocarcinoma. *Environ Toxicol*. 2024;39(12):5321–5333. doi:10.1002/tox.24407
10. Kuang L, Wang P, Zhou L, Li Y. Transformation of lung adenocarcinoma to small cell lung cancer following osimertinib treatment: a case report and literature review. *Anti-Cancer Drugs*. 2025;36(3):253–259. doi:10.1097/CAD.0000000000001686
11. Su L, Zhao J, Su H, et al. CircRNAs in Lung Adenocarcinoma: diagnosis and Therapy. *Curr Gene Ther*. 2022;22(1):15–22. doi:10.2174/1566523221666211202095258.
12. Xue C, Li G, Zheng Q, et al. The functional roles of the circRNA/Wnt axis in cancer. *Mol Cancer*. 2022;21(1):108. doi:10.1186/s12943-022-01582-0
13. Zhong P, Guo A, Wang L, Lin X, Feng M. Circular RNA CDK6 suppresses cervical cancer proliferation and metastasis by sponging miR-449a. *Bioengineered*. 2022;13(3):4885–4897. doi:10.1080/21655979.2022.2036898
14. Tang L, Ruan Y, Wang B, Zhang M, Xue J, Wang T. Erianin inhibits the progression of DDP-resistant lung adenocarcinoma by regulating the Wnt/β-catenin pathway and activating the caspase-3 for apoptosis in vitro and in vivo. *Hereditas*. 2024;161(1):48. doi:10.1186/s41065-024-00351-x
15. Wu S, Wang H, Pan Y, Yang X, Wu D. miR-140-3p enhances cisplatin sensitivity and attenuates stem cell-like properties through repressing Wnt/β-catenin signaling in lung adenocarcinoma cells. *Exp Ther Med*. 2020;20(2):1664–1674. doi:10.3892/etm.2020.8847
16. Zhang Y, Zhang Q, Chen H, Wang C. BCL9 promotes epithelial mesenchymal transition and invasion in cisplatin resistant NSCLC cells via β-catenin pathway. *Life Sci*. 2018;208:284–294. doi:10.1016/j.lfs.2018.07.023
17. Song JX, Wang Y, Hua ZP, et al. FATS inhibits the Wnt pathway and induces apoptosis through degradation of MYH9 and enhances sensitivity to paclitaxel in breast cancer. *Cell Death Dis*. 2024;15(11):835. doi:10.1038/s41419-024-07164-w
18. Li T, Yang XH, Shao MJ, Dong YX, Li LY, Lin CZ. Effectiveness and mechanism of cisplatin combined with PDT on human lung adenocarcinoma A549 cells transplanted tumor in nude mice. *Sci Rep*. 2025;15(1):10062. doi:10.1038/s41598-025-94990-3
19. Meyer CJ, Krauth M, Wick MJ, et al. Peloruside A Inhibits Growth of Human Lung and Breast Tumor Xenografts in an Athymic nu/nu Mouse Model. *Mol Cancer Ther*. 2015;14(8):1816–1823. doi:10.1158/1535-7163.MCT-15-0167
20. Nairuz T, Mahmud Z, Manik RK, Kabir Y. Cancer stem cells: an insight into the development of metastatic tumors and therapy resistance. *Stem Cell Rev Rep*. 2023;19(6):1577–1595. doi:10.1007/s12015-023-10529-x
21. Bryl R, Piwocka O, Kawka E, Mozdziak P, Kempisty B, Knopik-Skrocka A. Cancer Stem Cells-The Insight into Non-Coding RNAs. *Cells*. 2022;11 (22):3699. doi:10.3390/cells11223699
22. Chen X, Tang K, Li X, et al. Biomechanics of cancer stem cells. *Essays Bioochem*. 2022;66(4):359–369. doi:10.1042/EBC20220014
23. Yang Y, Li M, Zhou X, et al. PHF5A Contributes to the Maintenance of the Cancer Stem-like Phenotype in Non-Small Cell Lung Cancer by Regulating Histone Deacetylase 8. *Ann Clin Lab Sci*. 2022;52(3):439–451.
24. Babayev M, Silveyra P. Role of circular RNAs in lung cancer. *Front Genetics*. 2024;15:1346119. doi:10.3389/fgene.2024.1346119
25. Shibata M, Ooki A, Inokawa Y, et al. Concurrent Targeting of Potential Cancer Stem Cells Regulating Pathways Sensitizes Lung Adenocarcinoma to Standard Chemotherapy. *Mol Cancer Ther*. 2020;19(10):2175–2185. doi:10.1158/1535-7163.MCT-20-0024
26. Jin M, Liu X, Wu Y, Lou Y, Li X, Huang G. Circular RNA EPB41 expression predicts unfavorable prognoses in NSCLC by regulating miR-486-3p/eIF5A axis-mediated stemness. *Can Cell Inter*. 2022;22(1):219. doi:10.1186/s12935-022-02618-7
27. Paterson C, Kilmister EJ, Brasch HD, et al. Cell Populations Expressing Stemness-Associated Markers in Lung Adenocarcinoma. *Life*. 2021;11 (10):1106. doi:10.3390/life11101106
28. Zhou H, Tan L, Liu B, Guan XY. Cancer stem cells: recent insights and therapies. *Biochem Pharmacol*. 2023;209:115441. doi:10.1016/j.bcp.2023.115441
29. Chu X, Tian W, Ning J, et al. Cancer stem cells: advances in knowledge and implications for cancer therapy. *Signal Transduc Target Ther*. 2024;9 (1):170. doi:10.1038/s41392-024-01851-y

30. Aleksandrova KV, Suvorova II. Evaluation of the Effectiveness of Various Autophagy Inhibitors in A549 Cancer Stem Cells. *Acta naturae*. 2023;15(1):19–25. doi:10.32607/actanaturae.11891
31. Yu N, Gong H, Chen W, Peng W. CircRNA ZKSCAN1 promotes lung adenocarcinoma progression by miR-185-5p/TAGLN2 axis. *Thoracic Cancer*. 2023;14(16):1467–1476. doi:10.1111/1759-7714.14889
32. Cao L, Zhou X, Ding X, Gao D. Knockdown of circ-PVT1 inhibits the progression of lung adenocarcinoma and enhances the sensitivity to cisplatin via the miR-429/FOXK1 signaling axis. *Mol Med Rep*. 2021;24(4):684. doi:10.3892/mmr.2021.12323
33. Fan Z, Wang H. CircZSWIM4 facilitates tumor development in lung adenocarcinoma by targeting miR-370-3p and miR-873-5p to regulate the axis of FOXM1/β-catenin. *Cell Mol Biol*. 2023;69(6):132–140. doi:10.14715/cmb/2023.69.6.20
34. Geng J, Yang K. circCCND1 Regulates Oxidative Stress and FGF9 to Enhance Chemoresistance of Non-Small Cell Lung Cancer via Sponging miR-187-3p. *DNA Cell Biol*. 2021;40(5):675–682. doi:10.1089/dna.2020.6412
35. Yao Y, Zhou Y, Hua Q. circRNA hsa_circ_0018414 inhibits the progression of LUAD by sponging miR-6807-3p and upregulating DKK1. *Mol Ther Nucleic Acids*. 2021;23:783–796. doi:10.1016/j.omtn.2020.12.031
36. Shi H, Tan Z, Duan B, et al. LASS2 enhances chemosensitivity to cisplatin by inhibiting PP2A-mediated β-catenin dephosphorylation in a subset of stem-like bladder cancer cells. *BMC Med*. 2024;22(1):19. doi:10.1186/s12916-023-03243-5
37. Chen B, Zhang D, Kuai J, Cheng M, Fang X, Li G. Upregulation of miR-199a/b contributes to cisplatin resistance via Wnt/β-catenin-ABCG2 signaling pathway in ALDHA1(+) colorectal cancer stem cells. *Tumour Biol*. 2017;39(6):1010428317715155. doi:10.1177/1010428317715155
38. Roy S, Kar M, Roy S, et al. Inhibition of CD44 sensitizes cisplatin-resistance and affects Wnt/β-catenin signaling in HNSCC cells. *Int J Biol Macromol*. 2020;149:501–512. doi:10.1016/j.ijbiomac.2020.01.131
39. He J, Shi J, Zhang K, et al. Sox2 inhibits Wnt-β-catenin signaling and metastatic potency of cisplatin-resistant lung adenocarcinoma cells. *Mol Med Rep*. 2017;15(4):1693–1701. doi:10.3892/mmr.2017.6170
40. Guan C, Li X, Zeng X, et al. Unraveling the alterations and biomarkers in the tumor microenvironment in lung adenocarcinoma metastases and their indications for therapeutic response and prognosis. *Therapeut Adv Med Oncol*. 2025;17:17588359251403904. doi:10.1177/17588359251403904
41. Song L, Gong Y, Wang E, Huang J, Li Y. Unraveling the tumor immune microenvironment of lung adenocarcinoma using single-cell RNA sequencing. *Therapeut Adv Med Oncol*. 2024;16:17588359231210274. doi:10.1177/17588359231210274
42. Soler MF, Abaurrea A, Azcoaga P, Araujo AM, Caffarel MM. New perspectives in cancer immunotherapy: targeting IL-6 cytokine family. *J Immuno Ther Cancer*. 2023;11(11):e007530. doi:10.1136/jitc-2023-007530
43. Zhou Y, Qian M, Li J, et al. The role of tumor-associated macrophages in lung cancer: from mechanism to small molecule therapy. *Biomed Pharmacothe*. 2024;170:116014. doi:10.1016/j.biopha.2023.116014
44. Gao F, You X, Yang L, Zou X, Sui B. Boosting immune responses in lung tumor immune microenvironment: a comprehensive review of strategies and adjuvants. *Int Revi Immunol*. 2024;43(5):280–308. doi:10.1080/08830185.2024.2333275